AAS 95-382

EXPOSURE OF THE CASSINI SPACECRAFT TO HORSESHOE AND TADPOLE PARTICLE ZONES

Aron A. Wolf* and David A. Seal*

Regions called "horseshoes" and "tadpoles" exist along the orbits of Saturn's satellites, within which particles can be trapped by gravitational interactions of Saturn and the satellites. Although the extent of particle accumulation in these regions is not known, trapped particles might post? a hazard to the Cassini spacecraft. The amount of time spent in these regions is determined for several sample tours. Methods of reducing exposure time and effects of these methods on science return and mission operations are discussed. An estimate is made of how much time can be spent in these regions without incurring unacceptable risk.

INTRODUCTION

The Cassini spacecraft will fly a four-year orbital tour of Saturn and its moons, conducting an intensive investigation of the Saturnian environment. Flight is prohibited through the dense A, B, or C rings or the small F and G rings, due to the volume of hazardous material in these regions. The spacecraft will fly through the gap between the F and G rings only under controlled conditions which reduce the probability of impacting ring particles to low levels[1]. Ring plane crossings within the broader E-ring, which extends roughly from 3 to 9 Saturn radii (1-? S), arc permitted (in fact, they are necessary to achieve close approaches to several icy satellites whose orbits lie in this region). ii-ring particles arc estimated to be micron-sized[2], too small to cause damage to the spacecraft. However, no determination has yet been made of the necessity of avoiding the regions shape.d like "horseshoes" and "tadpoles" along the orbits of the satellites. A study of the spacecraft's exposure to these regions is undertaken here to aid in making this determination.

The principal objectives of the study arc to determine the amount of time the spacecraft is exposed to horseshoe and tadpole regions during several sample tours, to make a preliminary determination of the level of risk incurred as a consequence, and to find methods of reducing exposure time and consider effects these methods might have on science return or operational considerations.

Horseshoes and Tadpoles

For each individual satellite, the laws of motion of the "restricted three-body problem" apply. They treat the system of three. bodies as consisting of a major body (Saturn in our case), a minor body (a satellite moving about Saturn in a near circular orbit) and a nearly massless object (debris, spacecraft, etc.) whose gravity does *not* affect the motions of the two major players.

"Member of Technical Staff, Cassini Mission Design, Jet Propulsion Laboratory, Pasadena, California 91101.

The major bodies of such a system move about the system's barycenter. The massless body is constrained to lie outside certain boundaries in the planet-satclli(c space, depending on the value of the constant of integration C in the Jacobi integral:

$$V^2 = 2U - C \tag{1}$$

where

$$2U = (x^2 + y^2) + 2Gm_1/r_1 + 2Gm_2/r_2, \tag{2}$$

In the above equation, x and y arc the components of the particle's position, expressed in a two-dimensional, rotating coordinate system whose origin is at the barycenter and whose x-axis always points toward the center of the minor body; r_1 and r_2 arc the particle's distances from the major and minor bodies; and m_1 and m_2 arc the masses of the major and minor bodies. At a particular position (x,y), the greater the particle's velocity, the smaller the value of C associated with its motion.

Readers may wish to refer to Figures 1 and 2 during the following discussion. Figure 1 is a schematic diagram of the horseshoe and tadpole zones in the rotating coordinate system. Figure 2 presents "mro-velocity contours" for the Sun-Jupiter system, which provides a good illustration of some of the points **discussed below.**

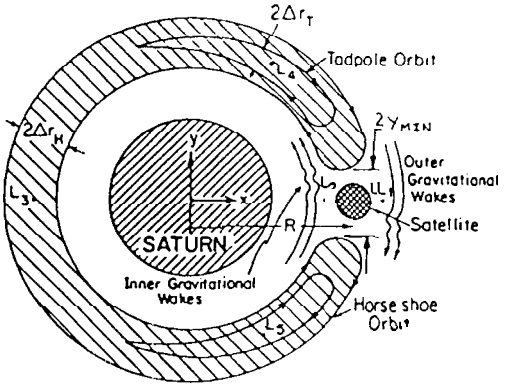

Figure 1 Tadpole and horseshoe regions in coordinate system rotating with Saturn-satellite line, 1.; arc Lagrangian equilibrium points.

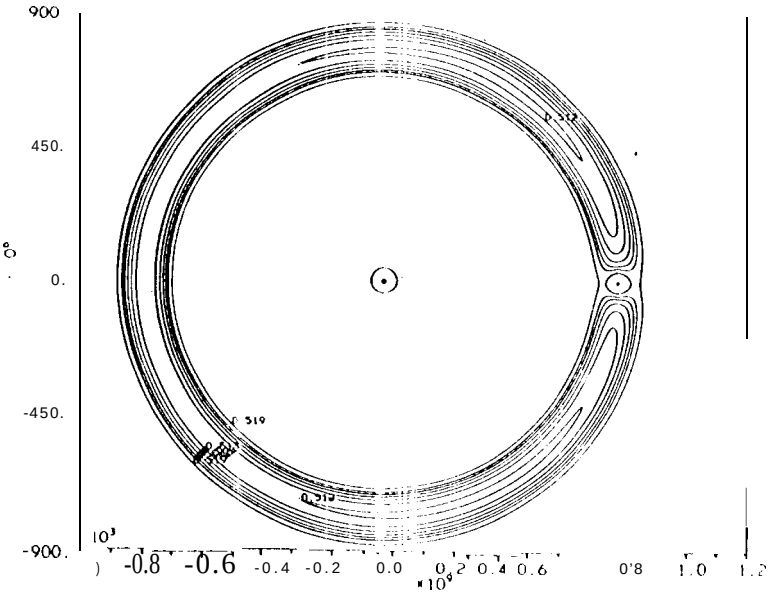

Figure 2 7.cro-velocity contours in the Sun-Jupiter system.

A z.cro-velocity contour can be drawn in the rotating reference frame for any value of C by setting $V = O$ in the above equation. Near either the major or the minor body, these contours arc circular and concentric, and C decreases with distance from the body. However, in the region near the satellite's orbit (but away from the satellite itself), they assume the characteristic horseshoe and tadpole shapes shown in tile figure.

Approaching the satellite's orbit from the direction of the major body, the contours break from their circular shape as C is reduced and assume the shape of a horseshoe with the satellite at the open end. As wc get closer to the satellite's orbit, with further decrease in C, the horseshoe narrows, and its length shrinks. Approaching closer, C decreases further until the horseshoe splits into two regions roughly shaped like tadpoles. These first appear to be joined at their tails at the L3 Lagrangian point (opposite the satellite's position). Contours of lower C appeal as progressively smaller tadpoles surrounding the two "I agrangian Equilateral Points." One of these points, labeled L4, leads the sate.llitc's position by a 60° angle; the other, labeled 1.5, trails by 60°. The tadpoles decrease in size as C decreases until local minima arc reached at the 1.4 and L5 Lagrangian points. 7.ero-velocity curves arc explained in greater detail in Refs. 3, 4, and 5.

A particle placed at L4 or L5 with zero velocity (in the rotating frame) stays there, because no resultant force acts on it. A small displacement (or the addition of a small velocity) causes the particle to Ii brate in the vicinity of the point. If the major body is at least 25 times more massive than the minor body (as is the case for Saturn and all its satellites), the motion in the vicinity of the 1A and 1.5 points is stable (i.e., the particle will not depart the vicinity of the L4 or L5 point). According to Dermott and Murray[5], the shape of the path along which such a particle librates closely corresponds to the shape of its associated zero-velocity curve, Numerical integrations of particle trajectories have been performed by Zhao and Liu4 which show that over long periods of time, particles travel within regions which resemble the horseshoe and tadpole shapes of the zero- velocity curves.

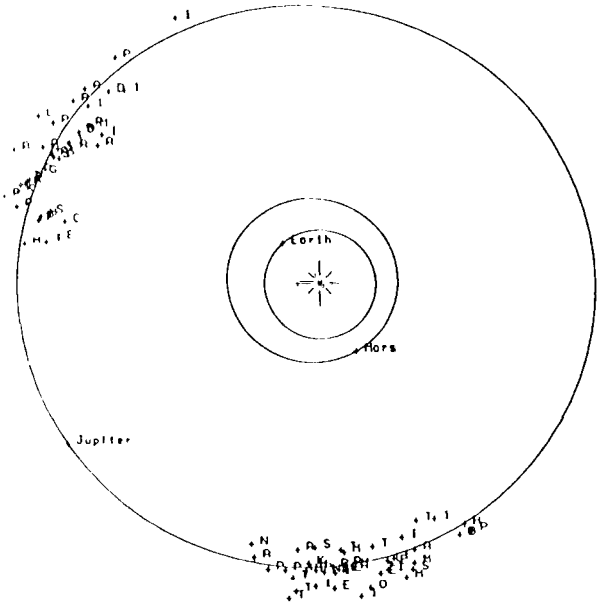

Figure 3 The orbit of Jupiter + 80 Trojans (epoch: February 1, 1994)

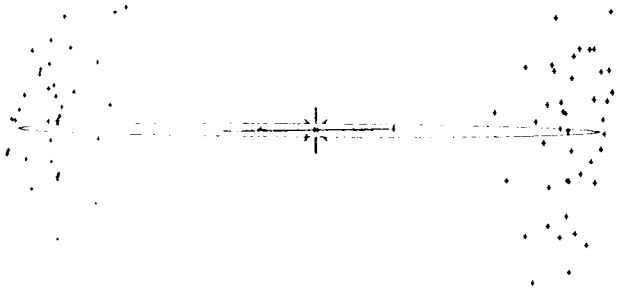

Figure 4 The orbit of Jupiter + 80 Trojans, edge view (epoch: February 1, 1994)

The largest horseshoe contour separates the concentric contour sets about each body from the horseshoe/tadpole region. At its open end, near the satellite, the inner and outer branches rejoin and c1osc off, forming a nearly spherical region about the satellite. It appears that this region near the satellite is a "clear zone," continuously cleared of possible Saturnian system debris by chaotic particle motion. The effect of bodily sweeping particulate matter out of a trajectory "tube" is a complex n-body process. Indeed, the entire horseshoe/tadpole construct is based on the restricted three-body problem, which fails to take into account gravitational effects of more than onc satellite and non- gravitational forces upon the particle.

These interactions are complex, and further work must be undertaken to fully understand them.

Debris population in horseshoe/tadpole regions

Nature does indeed display examples of captured objects in such regions, the most famous being the "Trojan Satellites" of Jupiter, clearly observable through telescopes. These objects arc asteroids, captured by the planet Jupiter to lead or follow it in its orbit at the 60° equilateral Lagrangian points. Figures 3 and **4** graphically depict this tadpole capture phenomenon, plotted by Bender[7].

An overlay of Figures **2** and 3 (which were intentionally produced at the same scale) shows that the actual population of objects at the epoch of the. plot extends beyond the boundaries of the tadpole region. This shows that the actual captured material distribution may not strictly conform to the restricted three-body model, but is definitely held in a pack centered on the L4 and L5 points. There arc at present 184 Trojan asteroids known. '1'heir diameters must exceed about 10 km in order to be visible from Earth. The amount of smaller debris is not known.

Another three examples of L4/L5-type debris were discovered in the Saturnian system during the Voyager I flyby [8]. These are Satellite 1980 S 13 at the L4 point of Tethys, Satellite 1980 S25 at the L5 point of Tethys, and Satellite 1980 S6 at the 1.4 point of Dione. These discoveries arc clear warning signs that debris exists and gravitational interactions can keep these small Saturnian satellites permanently anchored to their bigger satellite neighbors.

in addition, small, perhaps microscopic debris has been shown to exist in the so-called E ring (called the D ring in original discovery papers[9]). During opportunities to view Saturn's rings edge-on from Earth, the E ring showed up photographically as a fuzzy haze extending from about three to nine Saturnian radii (RS), encompassing the realm of the five icy satellites of Saturn (Mimas, Enceladus, Tethys, Dione and Rhea). Maximal thickness was observed at the orbit of Enceladus, the satellite with the youngest, smoothest surface structure of the sets. It is conceivable that this satellite, positioned in the middle of the group, experiences the strongest tidal effects and supports volcanic geyser activity, with part of the eruptions escaping Enceladus and merging into the E ring. The frozen droplets of unknown size may in fact form the bulk of the observed E-ring haze[10,11,12,13].

Radially narrow magnetospheric depletions known as "microsignatures" also provide some evidence of the coalescence of particles in the satellites' orbits. These microsignatures have been observed by Pioneer and Voyager in the orbits of Mimas, Enceladus, Tethys, Dione, and Rhea (but not Titan), and have been generally attributed to clumpy material which may be sporadic or somehow shepherded. The material may be of concern to the spacecraft, although it has low optical depth which probably defies dire.ct imaging.

Particle Models

A number of investigators have worked on the particle size distribution problem. Neil Divine's extensive work at JPL[14] summarized the then available information and proposed three distribution models of varying conservatism These models are based primarily on imaging data from Earth at Saturn's ring plane crossings in 1980 and data from the Voyager 1 and 2 flybys in 1980 and 1981. Several distributions are. considered, from "nominal" conditions to more conservative wors[-case estimates, where intermediate-si~,ed particles dominate the population of particulate matter. Of pi imary interest arc the particles of $1 ()^{-4}$ to $1 ()^{-2}$ grams which can damage critical spacecraft surfaces such as the main engine, propellant tanks or the electronic bus. Less massive particles are also of interest in evaluating optical surface degradation and measurement by science instruments.

Divine's small and intermediate particle models have been used to assess risk. In the small particle model, the mass and number of particles are concentrated in the smaller sizes. The intermediate model predicts most of the mass is in the medium to large particle sizes, though the smaller particles still dominate in numbers. Divine also includes a large particle model, but this is not included in the present analysis. In this model the mass and number of particles is concentrated almost exclusively in the large sizes. Mot-c recent work[2] has shown (his is highly unlikely.

Divine's models treat the ring plane as homogeneous, and do not include any variation in particle density in horseshoe or tadpole regions. Models of particle densities specific to these regions are difficult to develop because of the almost complete lack of data on the regions. The range of distances covered by Divine's models includes the main inner icy satellites. Presumably, the material trapped in satellite orbits is similar in nature to the material predicted by the models to be near the satellite's orbit, perhaps having been trapped over time through a variety of dynamic processes.

in this analysis, Divine's models are used directly to compute fluences and hit probabilities for the trapped particle regions around these icy satellites. For conservatism, a somewhat arbitrary factor of 10 scaling in fluence is applied to the tadpole regions. No scaling is applied to the larger horseshoe. regions. The models are applied to Titan orbit crossings as well as those of the icy satellites, even in the absence of microsignatures. Efforts to improve modelling of particle densities in horseshoe and tadpole regions are ongoing.

Divine's ring-plane theory models the ring planes as Gaussian distributions with thicknesses and particle size distributions varying with distance from Saturn. For spacecraft traveling through these areas it is appropriate to model particulate concentration in terms of the number of particles larger than a certain size per unit volume. This is logical because particles of any size exceeding the mass threshold for a spacecraft subsystem are of concern.

I'article distributions have been expressed by Divine as logarithmic functions containing the mass threshold of the component of interest as follows:

$$\log p_a = C_1 + C_2 \log m \tag{3}$$

where p_a represents a size distribution and C_1 and C2 are constants determined from particle zone observations. I lere m is the minimum par title mass which causes failure of the vulnerable subsystems. The threshold mass m depends on the nature of the component as well as the speed of the particle, and is given by:

$$\log m = \log m_o + \beta \log V \tag{4}$$

where V is the spacecraft-relative particle velocity in km/see and m_0 and β are determined from the material and construction of the subsystem.

The following tables (1 and 2) describe the mission-critical failure modes which may be caused by particle impacts on the Cassini spacecraft. Particle impacts on the last two subsystems (shunt radiator and RTGs) cause degradation of the mission, but not mission failure. Table 2 contains the effective areas and mass thresholds for these subsystems.

Variables which contain the subscript "a" are relevant to those particles greater in mass than m above. For these studies, the density of all particles is assumed to be approximately that of water (1 g/cm^3). With this fixed-density assumption, mass (m) and size (a) distributions have a one-to-one correspondence.

Table 1
SUBSYSTEMS VULNERABLE TO PARTICLE IMPACT-FAILURE MODES

Subsystem	Failure Mode	Failure Result
Bipropellant tanks	puncture tank	loss of propulsion
Hydrazine tank	puncture tank	no RWA unloads; loss of attitude control
Pressurant tank	puncture tank	PMS in blowdown node
Main engines	damage nozzle coating	engine unusable; burn-through
Bus (MLI)	pierce shear plate	loss of electronics in bay
Bus (Louv no cv)	pierce shear plate	loss of electronics in bay
Bus (Louv w/cv)	pierce shear plate	bss of electronics in bay
Shunt radiator'	damage heater circuits	degradation of power output
RTGs*	damage thermocouples	loss of power output

' Degradation, not mission failure.

Table 2
SUBSYSTEMS VULNERABLE TO PARTICLE IMPACT-AREAS & THRESHOLDS

Subsystem	Max. Area (m^2)	log mo (g)	b
Bipropellant tanks	3.17	--0.523	**–1.000**
Hydrazine tank	**0.20**	**--0.824**	**-1.000**
Pressurant tank	0.32	**--1.'222**	**–1 .000**
Main engines	**0.20**	-2.960	**–1** .080
Bus (MLI)	**0.65**	**-1.144**	-1.322
Bus (Louv no cv)	**0.39**	**-1.144**	**-1.322**
Bus (Louv w/cv)	**0.26**	-0.691	**-1.152**
Shunt radiator	**0.66**	**-1.574**	**-1.807**
RTGs	**0.22**	**1.803**	**-2.515**

The concentration of particles greater than a certain size a is 'expressed in Divine's models as:

$$N_a = \kappa p_a \frac{e^{-(z^2/2\sigma_z^2)}}{\sigma_z 42^{-}\overline{\pi}^{-}} \qquad \text{(s)}$$

where Na is the particle concentration (number of particles greater than size a per cubic meter), κ is the particles' geometric cross-section per unit area, z is the height from the equatorial plane, σz is the height parameter of the Gaussian distribution, and pa is the cumulative size distribution of particles in m–2. Divine's models account for the selection of κ, pa and σz, which all vary with distance from Saturn. Furthermore, pa varies with choice of a mass threshold determined by the vulnerability of individual subsystems to particles. The path of the spacecraft (which determines z as a function of time) is integrated in a later step. The particle flux is then computed:

$$J_a = \eta V N_a \qquad \textbf{(6)}$$

where Ja is the particle flux (number of particles per m2 - second), V is the speed of particles with respect to a spacecraft surface, and η is the weighting function based on how the surfaces arc oriented with respect to the incoming particle. 1 'or simplicit y, η has been assumed to be I (i.e., all surfaces arc faced directly into the particle stream).

Fluences, expressed as the number of particles expected per square meter of exposed spacecraft area, can now be calculated:

$$F_a = \int_{t_1}^{t_2} J_a dt \tag{7}$$

which integrates the path of the spacecraft through the particle region from time t_1 to **12.** The integral can be rewritten in terms of the distance z from the ring plane or z calculated as a function of time.

Fluences are calculated for each spacecraft subsystem, summed for all horseshoe and/or tadpole zone crossings, and combined with the areas of the subsystems to produce a total impact probability (assuming a Poisson distribution) for a set of zone crossings:

$$P = 1 - e^{-\sum_i (AF_a)_i} \tag{8}$$

where A is the subsystem area and Fa is the sum of fluences of particles greater than size a.

Dimensions of horseshoe and tadpole regions

A number of researchers attempted to assess the width of the horseshoe and tadpole bands and their structure in and out of the orbital plane of the major two bodies[5, 8] The last set of horseshoe/[adpolc characteristic sizes was produced by Burns, Kolvoord and Hamilton[15] and later re-evaluated and confirmed by Divine[6]. These values are shown in Table 3. These authors used formulations more complex than the restricted three-body problem, and the zone widths they computed are somewhat smaller than those obtained using the restricted three-body for-mu lation. It is possible that effects remain which are still unaccounted for in any of these references (such as gravitational interactions between the satellites) which may alter the result,

Table 3
DIMENSIONS OF HORSESHOE, TADPOLE, AND CLEAR ZONES
(See Figure 1 for illustration)

SATELLITE	TADPOLE RADIUS Dr_t (KM)	HORSESHOE RADIUS Dr_h (KM)	CLEAR ZONE y_{min} (KM)
Mirnas	55	375	7500
Enceladus	101	614	12055
Tethys	355	1520	28000
Dione	590	2300	41000
Rhea	1230	4200	71000
Titan	22000	38000	450000

STUDY METHOD

The principal source of the results presented here. is the STOUR program, which is used in the initial 'stages of tour design. STOUR uses a "zero sphere-of-;nfruence patched conic" algorithm, in which both Saturn-centered and satellite-centered orbits are propagated using two-body conic methods and then "patched" together to create an approximation of a tour trajectory. Trajectory propagation is fast, but some accuracy is sacrificed for speed.

The ability to model horseshoe and tadpole regions in a rudimentary fashion was incorporated into STOUR. The model makes several simplifying assumptions, illustrated in Figure 5. The regions are assumed to be sections of a torus with a circular cross-section. A horseshoe region is modeled as a torus with a "chunk" taken out in the vicinity of the

satellite (representing the clear zone). Tadpoles arc sections of a torus in the vicinity of either the L4 or L5 libration points. (For simplicity, STOUR does not model the characteristic "tadpole" shape of these regions, thus overestimating the spacecraft's exposure to tadpole regions.) The values listed in Table 3 arc used to define the horseshoe. and tadpole regions for Saturn's innermost six satellites. This toroidal model dots not take. the eccentricity of the satellites' orbits into account. The torus is centered on a circle whose radius is equal to the satellite's average orbital radius.

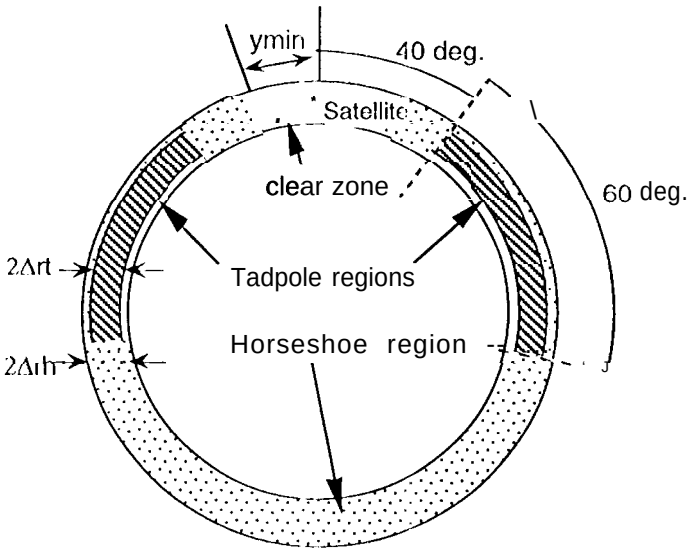

Figure 5 **STOUR horseshoe and tadpole zone modeling**

Given the current state of our knowledge about these regions, these assumptions are not believed to be crippling. However, neither should they be considered accurate for an individual tour. Any sample tour trajectory presented here would change if submitted to the optimization and integration process, and the amount of time spent in horseshoe and tadpole regions would change as a result. Also, adoption of more detailed horseshoe/tadpole models would alter the amount of exposure for an individual tour. Nevertheless, we believe that the results of this study are adequate to form certain conclusions about exposure to these regions for different types of tours which arc not materially affected by the inaccuracy of these assumptions.

In order to accomplish these objectives, six sample tours (numbered I through 6) were evaluated for exposure to horseshoe and tadpole regions.

RESULTS

Results obtained from STOUR for all six sample tours are discussed here., but in the interest of brevity, graphic illustrations are included here only for two tours (1 and 6). These are shown in Figures 6 and 7. Because Mimas, Enceladus, Tethys, Dione, and Rhea arc within the E-ring and Titan is not, we have chosen to present the data for Titan separately from these inner icy satellites. Five plots are included for each sample tour. The first two show the time spent (iii minutes) in the inner icy satellites' horse.shoe and tadpole regions between each flyby and the next (e.g., "T1" signifies the leg between Titan 1 and Titan 2). (Note that a trajectory segment between two flybys often consists of more than onc revolution around the planet !). The next two plots show the time spent in Titan's horse.shoe and tadpole regions. The last plot shows the orbital inclination profile thi oughout the tour.

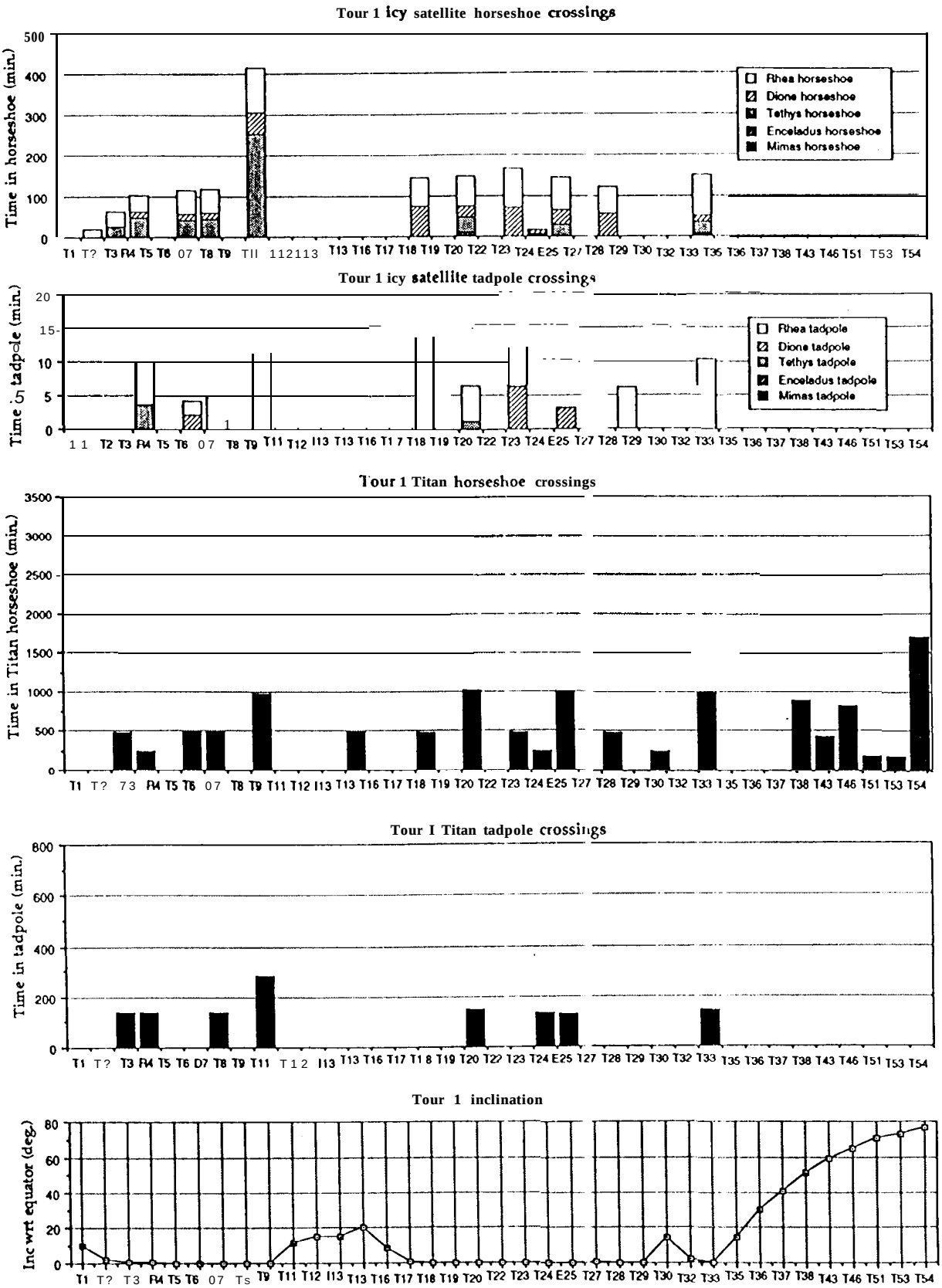

Figure 6 IlorsMloc/tadpole crossings and inclination, tour 1

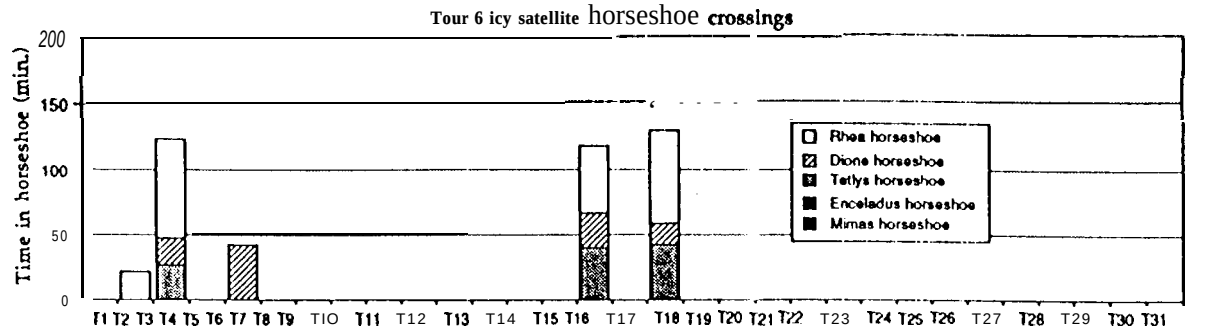

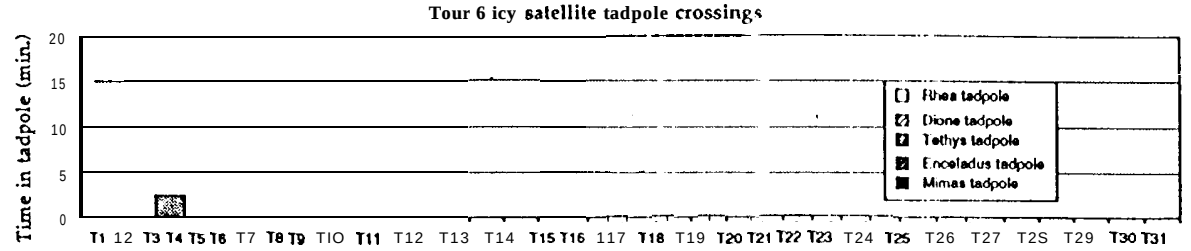

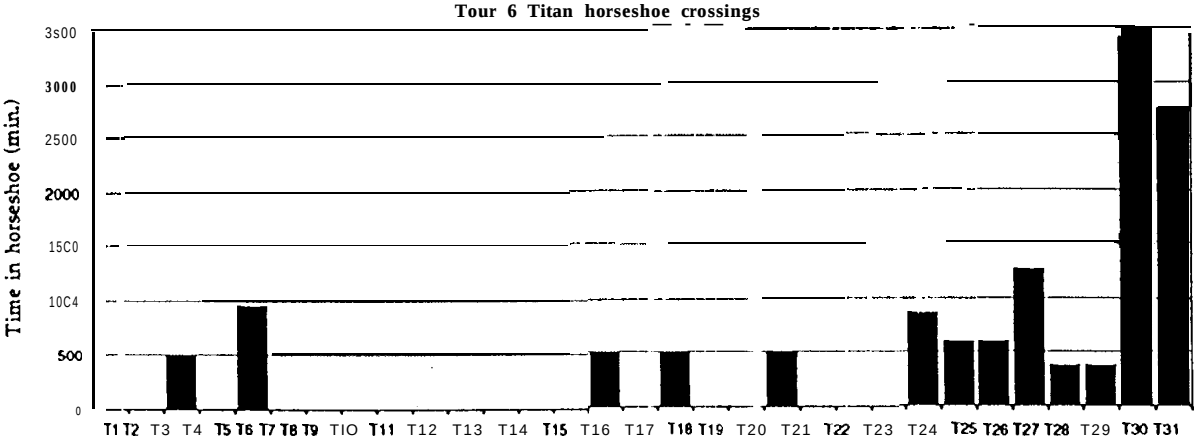

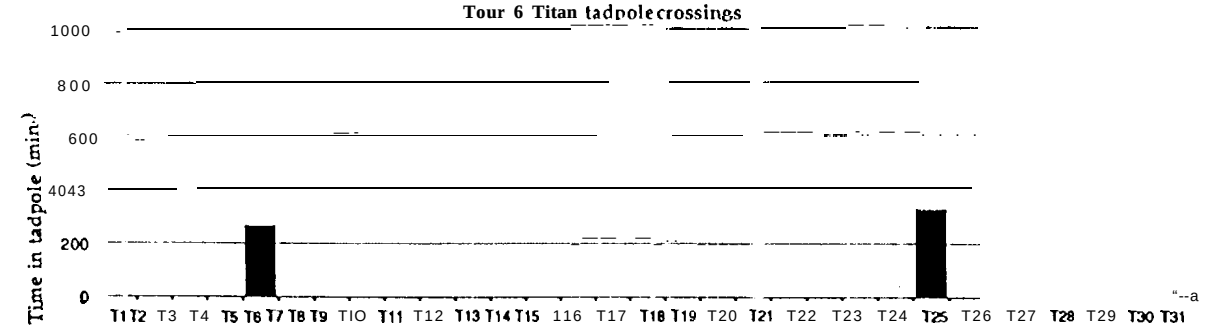

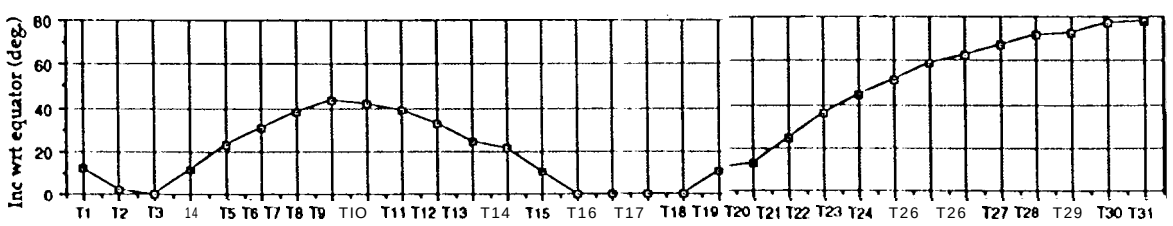

Figure 7 IIorscslloc/tadpole crossings and inclination, tour 6

A summary of horseshoe ant] tadpole exposure times (in hours) for all six tours by satellite, is shown in Table 4.

Table 4
HORSESHOE AND TADPOLE CROSSING DURATIONS (IN HOURS) BY SATELLITE

HORSESHOES

	Mimas	Enceladus	Tethys	Dione	Rhea	TOTAL ICY SATS	Titan	TOTAL ALL SATS
Tour 1	0.00	0.29	8.43	6.71	13.23	28.67	204.11	232.79
Tour 2	0.00	0.00	0.44	4.50	6.96	11.90	76.79	88.69
Tour 3	0.00	0.00	0.44	3.90	6.31	10.65	195.03	205.68
Tour 4	0.00	0.00	0.00	5.68	9.98	15.67	109.94	125.61
Tour 5	0.00	0.00	5.17	3.74	11.59	20.50	170.37	190.87
Tour 6	0,00	0.00	1.82	1.77	3.61	7.20	218.72	225.92

IADPOLES

	Mimas	Enceladus	Tethys	Dione	Rhea	TOTAL ICY SATS	Titan	TOTAL ALL SATS
Tour 1	0.00	0.00	0.08	0.19	1.07	1.35	40.17	41.52
Tour 2	0.00	0.00	0.04	0.03	0.22	0.30	6.71	7.01
Tour 3	0.00	0.00	0.04	0.00	0.19	0.23	25.28	25.51
Tour 4	0,00	0.00	0.00	0.04	0.32	0.36	14.27	14.63
Tour 5	0.00	0.00	0.17	0.09	0.34	0.59	17.40	17.99
Tour 6	0.00	0.00	0.04	0.00	0,00	0.04	45.01	45.05

As the table shows, neither the horseshoe nor the tadpole zone of Mimas is penetrated during any of the sample tours. Enceladus' horseshoe is penetrated only in tour 1, for a total of 18 minutes; its tadpole zone is not penetrated at all. This is because the periapse of the spacecraft's orbit rarely dips below the orbits of either of these two satellites.

The spacecraft spends roughly an order of magnitude more time in Titan's horseshoe and tadpole zones than in those of the inner icy satellites. '1'here arc three reasons for this. First, Titan's z.ones arc larger. Second, the spacecraft is further from periapse, and traveling more slowly, near Titan. Third, the number of crossings of Titan's zones in a tour can be greater than that of the inner icy satellites' zones because Titan zonal crossings can occur at any inclination, whereas crossings of the inner icy satellites' zones occur typically at low inclinations only. Reasons for this arc explained in greater detail later.

Time spent in the tadpoles is 1-'2 orders of magnitude less than time spent in the horseshoes. For comparison, the total volume of both of Titan's tadpole zones is 9.8% of the volume of its horseshoe zone.

Impact probabilities assuming both one. and two intact main engines at the start of the. tour were calculated for each sample tour using Divine's models. These are quite low. The largest impact probability for two engines intact is 2x 10-6 (for Tour 1); for one engine intact, the largest probability is $2x\ 10^{-5}$ (also for Tour 1). Although impact probabilities arc small, the inadequacies and uncertainties of the current models arc large enought that a conservative

approach is required. An investigation of strategies of avoiding horseshoe and tadpole z.ones is a necessary part of such a conservative approach.

The plots show that zone passages occur only on some legs, *while* other orbits arc completely free of such passages. During portions of tours, a repeating cycle exists in which significant horseshoe zone exposure shows up every other trajectory leg with no exposure on alternating legs. In other portions of tours, the spacecraft flies for several orbits without any horseshoe passages at all. An explanation of the reasons for the existence of these patterns is a first step in considering methods of avoiding the zones.

Horseshoe crossings in near-equatorial orbits

When the spacecraft's orbital inclination is within a degree or two of Saturn's equator, the spacecraft passes through the horseshoe (or clear zone) of any satellite whose orbital radius is between the spacecraft's apoapse and pcr iapse. Figure 8 shows schematically how horseshoe exposure time can accumulate on a single trajectory leg between two flybys. As is typical throughout large portions of the sample tours, the spacecraft's apoapse in this example is beyond Titan's orbit, and its periapse is below the orbit of Dione. As the spacecraft proceeds inbound from apoapse, it traverse.s the horseshoe zones of Titan, Rhea and Dione. All these zones arc traversed again on the outbound leg after periapse.

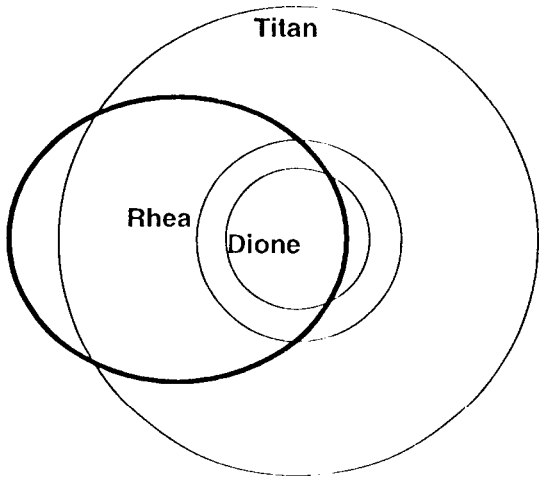

Figure 8 Typical low-inclination orbit, showing several horseshoe crossings

Furthermore, a leg between two flybys often contains more than one complete revolution. For example, the Titan 18 flyby of tour 1 is inbound, and Titan 19, an outbound flyby, occurs about 1-1/2 revolutions later. Two periapse passages, but only onc apoapse passage, take place between these two flybys. Dione's horseshoe is crossed four times (inbound and outbound for each periapse passage) Rhea's three times, and Titan's twice (inbound and outbound for each apoapse passage). Rhea's *orbit* is actually crossed four times, but a nontargeted flyby of Rhea occurs at onc of the crossings. The spacecraft passes through the clear zone CLOSC to the satellite, and enters neither the horseshoe nor the tadpole zones. Thus, when several revolutions take place between two flybys, many horseshoe crossings can occur between them. The sequence and durations of crossings on this leg is shown in Table 5.

Other legs contain less than onc complete revolution, and no periapse passages. For example, in tour 1, the Titan 17 flyby is outbound, and the Titan 18 flyby is inbound, with less than onc revolution between them. No passages through the inner icy satellites'

1VM'SCS}1OCS occur on such legs, because the spacecraft is always outside the orbits of the inner icy satellites.

Table 5
SEQUENCE AND DURATION (IN MINUTES) OF ZONE CROSSINGS, T18-T19 TRAJECTORY LEG, TOUR 1

SATELLITE	HORSE-SHOE	TAD-POLE	SATELLITE	HORSE-SHOE	TAD-POLE
(Titan 18, Inbound)			(Apoapse)		
RHEA	22.3		TITAN	**239.5**	
DIONE	29.0		(Rhea nontargeted - pass thru clear zone)		
(Periapse)			DIONE	29.0	
DIONE	8.5		(Periapse)		
RHEA	23,5	6.9	DIONE	8.5	
TITAN	239.5		RHEA	23.5	6.9
			(Titan 19, Outbound)		

The plots show a repeating cycle of significant horseshoe exposure on one trajectory leg alternating with none on the succeeding leg in portions of some tours. This pattern is associated with a sequence of targeted flybys used to rotate the line of apsides of the spacecraft's orbit. Orbit rotation is accomplished by changing period at a targeted flyby, and is necessary to allow the spacecraft to sample different regions of Saturn's magnetosphere and to achieve diverse viewing geometries of Saturn and its satellites. The direction of rotation depends on whether the flyby increases or decreases period and whether it is inbound or outbound[17].

Continuous clockwise rotation is produced by alternating inbound, period-increasing flybys with outbound, period-reducing ones. Counter-clockwise rotation is produced by alternating inbound, period-rcclucing flybys with outbound, pctiod-increasing ones. In bo(h of these scenarios, inbound-to-outbound legs (with more than one complete revolution, two periapse passages, and significant horseshoe exposure) alternate. with outbound-to-inbound legs (with less than onc complete revolution, no periapse passages, and no horseshoe exposure).

A flyby sequence of this type requires near-equatorial inclination. The plane of the transfer orbit between any two flybys is formed by the Saturn-centered position vectors of the satellites at the two flyby times. If the angle between the position vectors is other than 1800 or 360°, the orbital plane formed by the two vectors is unique, and lies close to Saturn's equator. So, for inbound-o utbound or outbound-inbound transfers, inclination must be near zero unless the transfer angle is I 80° (which is not usually the case).

Horseshoe crossings in high-inclination orbits

A comparison of the inclination profiles and zone crossing duration plots for the sample tours shows that exposure to the zones of the inner icy satellites is greatest at low inclinations and rarely occurs at inclinations above a few degrees. This is because the radii of the zones are small, and because they arc located near the satellites' orbit planes, which arc close to Saturn's equator. An inclination of a few degrees is sufficient to displace the spacecraft vertically out of the zones unless one of the two nodes (the points where the spacecraft crosses the equatorial plane) occurs at the orbital distance of onc of the satellites. If a nodal crossing dots occur at the orbital distance of onc of the satellites, a horseshoe passage occurs regardless of inclination unless the spacecraft is C1OSC enough to the satellite to be in its clear zone.

The plots show that crossings of the horseshoe and tadpole zones of Titan, unlike those of the inner satellites, occur at high as well as low inclinations. This is because one of

the two nodal crossings on every orbit must occur at the orbital radius of Titan, due to the integral role Titan flybys have in any Cassini tour. The spacecraft is always either coming from m going to a Titan flyby (or both), which means crossings of Titan's orbit occur on every revolution, whether or not Titan is nearby at the time. in what may seem a paradox, crossings of Titan's zones occur cm revolutions which do *not* contain Titan flybys. On revolutions containing Titan flybys, the spacecraft passes close enough to Titan to be in the clear zone, and no zone passage occurs.

Given that one node always occurs at Titan's orbit, it is possible to calculate the spacecraft's distance from Saturn at the other node for any combination of period and periapse radius. This information can be used to avoid combinations of period and periapse which place a node at the orbital radius of any of the inner icy satellites, which allows us to usc inclination to stay out of these zones entirely.

It is then possible to avoid situations like the one on the leg from Titan 5 to Titan 6 of tour 6. On this leg, five crossings of Dione's horseshoe, totaling 42 minutes, occur (one for each of five periapse passages between the two Titan flybys) even though the inclination is almost 23°. Using a different period/pcriapsc combination, all five could be avoided.

Tadpole crossings

For this study, each of the two tadpole regions associated with each satellite was assumed to extend over a 60° arc (from 40° to 100° from the satellite's position), as shown in Figure 5. The radii of the tadpole regions are smaller than the horseshoes (i.e., the tadpoles arc entirely contained within the horseshoes). A horseshoe crossing which occurs within the angular and radial limits of a tadpole region is a tadpole crossing as well.

Like horseshoe crossings, tadpole crossings which occur at low inclinations can be eliminated by increasing inclination, provided they do not occur at a node. Crossings at nodes occur even at high inclinations, and cannot be eliminated unless the node is moved. It is often possible to move the node away from the orbit of onc of the inner icy satellites. However, because of the frequency of Titan flybys in the tour, it is not often feasible to move a node away from Titan's orbit. Furthermore, resonance of the spacecraft's orbital period with Titan's gives rise to a regularity in the occurrence of Titan tadpole crossings. Crossings of the inner icy satellites' tadpoles occur with no such regularity, because the orbital periods of these satellites arc not commensurable with that of Titan.

The trajectory leg between Titan 8 and Titan 9 of tour 4 illustrates how passages through Titan's tadpole regions arc inevitably associated with certain resonances. These two flybys are both outbound. Between them, the spacecraft completes five full revolutions and Titan completes eight. Inclination is 20° The descending node occurs at Titan's orbit, and the ascending node is at 5.5 RS, between the orbits of Tethys and Dione (and outside horseshoe **and** tadpole zones). The spacecraft's period is approximately 25.5 days (1.6 x Titan's orbital period). During each complete spacecraft revolution, Titan travels 216° further around Saturn than the spacecraft. The spacecraft crosses Titan's orbit at a point 144° ahead of Titan after the first spacecraft revolution, 70° behind after two revolutions, 72° ahead after three revolut ions, and 145° behind after four revolutions. These crossing points are spaced evenly around Titan's orbit. The second and third crossings fall within the angular limits of tadpole zones (see also Figure 5). This geometry occurs whenever five full spacecraft revolutions take place between flybys, regardless of orbit period.

Similar analysis may be used to examine other situations in which integral numbers of spacecraft revolutions occur between flybys. Table 6 shows the number of Titan tadpole crossings expected for up to nine complete spacecraft revolutions between flybys.

The table shows that, in high inclination orbits, Titan tadpole crossings can be avoided if the spacecraft never travels more than three complete revolutions between Titan flybys, and

that crossings are inevitable if four or more spacecraft revolutions occur between ']"it,, flybys.

Table 6
NUMBER OF TITAN TADPOLE CROSSINGS EXPECTED BETWEEN FLYBYS

# S/C Revs	# Tadpole Crossings	# S/C Revs	# Tadpole Crossings
2	0	6	2
3	0	7	2
4	2	8	4
5	2	9	4

STRATEGIES OF AVOIDING THE INNER ICY SATELLITES' ZONES

The most obvious way to avoid the inner icy satellites' zones is to keep inclination high enough to avoid them throughout the entire tour (while also making sure the spacecraft does not cross the equator near the orbits of any of these satellites). This has the side-effect of reducing the number of opportunities available for icy satellite. encounters, because these opportunities are much more plentiful when the spacecraft orbits near the equator.

Alternate strategies can be used in which inclination is kept high at the beginning of the tour while in-situ observations of the Saturnian environment are made to better evaluate the debris hazard. Inclination can then be lowered to near the equator if the risk of doing so is determined to be acceptable. The project could retain the option of redesigning the tour to keep inclination high if the risk is found to be unacceptable.

Inclination can be kept above a few degrees either by using transfers of 180° or 360° or by incorporating "broken-plane" maneuvers into the tour. If the transfer angle between two flybys is either 360° (i.e., two flybys occur at the same place) or 180°, an infinite number of orbital planes connect the flybys. In this case, the plane of the transfer orbit can be inclined significantly to Saturn's equator. We can also say that if inclination is more than a few degrees, the transfer angle between the two Titan flybys forming the orbital plane *must* be nearly 180° or 360° (or an integer multiple. thereof).

Broken-plane maneuvers can be used for transfer angles other than 180° or 360°, expending propellant to raise the inclination of orbits which otherwise would be near-equatorial. Such plane-changing maneuvers are typically executed near apoapsis where the spacecraft's speed is slowest. The two methods can be combined. with portions of the tour consisting solely of 180° or 360° transfers and other portions containing broken-plane maneuvers. Each choice has consequences which can be explored.

Transfers of 180° or 360° only

Titan-Titan ransfers of 180° can only occur if both the ascending and descending nodes occur at the Titan's orbital radius[18]. This restricts their use to a specific set of orbital geometries which occur infrequently in tours. In a tour consisting only of 180° and 360° transfers, most of the legs are 360° transfers, with few 180° transfers. Tour 6 contains one 180° transfer and several 360° transfers.

The type of flyby sequence typically used to rotate the orbit (alternating inbound/outbound flybys coupled with alternating increase and decrease in period) cannot be used in a tour consisting only of 180° or 360° transfers. The transfer angles in such sequences are not near 180° or 360°. In tours containing only 180° or 360° transfers, most of the orbit rotation results from the few 180° transfer orbits, each of which can accomplish over 90° of rotation. A tour containing two 180° transfers covers about half the magnetosphere, with most of the coverage taking place during the relatively short amount of time spent on the

two 180° transfer legs. Transfers of 360° accomplish essentially no net orbit rotation. (The orbit is rotated as a consequence of any change in inclination, but its orientation is returned to the original value if inclination is reduced to its original value.)

Tours of only 180° or 3600 transfers do permit exploration of the full range of inclinations.

Use of broken-plane maneuvers

1 Iow much must inclination be raised in order to avoid the horseshoe and tadpole zones, and what is the AV cost of doing so? A sample trajectory leg (the leg from Titan 19 to Titan 20 of tour 2) was investigated in order to obtain preliminary estimates of the answers to these questions. Titan 19 is inbound, and Titan 20 is outbound, with two periapse passages and onc apoapse passage between them. The orbital period is 39.1 days. Without a maneuver to change inclination, four crossings of Rhea's and four of Dione's horseshoes totaling 145 minutes occur on this leg. Rhea's tadpole is crossed twice, for a total of 10 minutes. The results of the investigation arc shown in Figure 9. Inclination must bc raised to about 0.5° to eliminate tadpole zone crossings, which costs about 10 m/s. Both horseshoe and tadpole crossings can bc eliminated by raising inclination to about 2°, which requires an expenditure of **40** to **50** 01/s.

What is the AV expenditure for each sample tour if broken-plane maneuvers are added to completely avoid the icy inner satellites' horseshoe and tadpole zones for the entire tour? Figure 6 shows that for tour 1, there are 13 revolutions on which crossings of the inner icy satellites' 7.ones occur, represented by the 13 vertical bars on the horseshoe plot, (Since the tadpole regions arc embedded within the horseshoes, tadpole crossings occur only on legs in which horseshoe crossings occur.) Two of these legs contain crossings of much shorter duration than the otbcr 11. If wc assume a 40 m/s maneuver is needed on each of those 11 legs and a 20 m/s maneuver is needed on the two legs with short-duration crossings, the total AV cost is 480 m/s for 1.

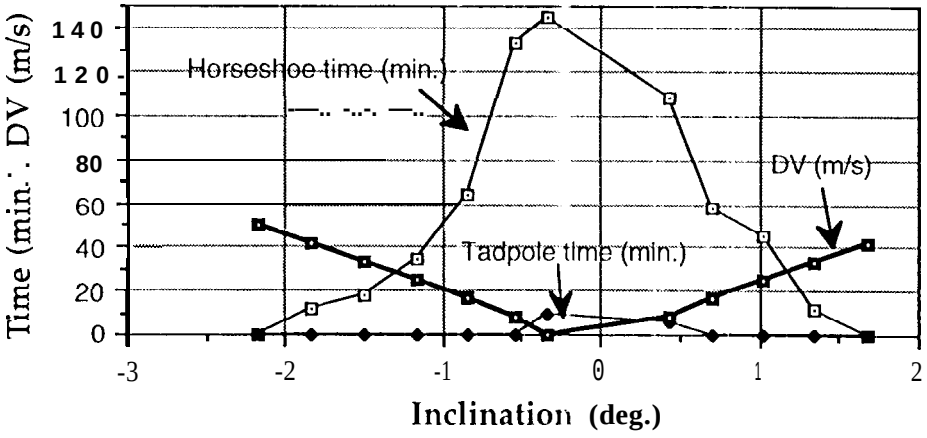

Figure 9 Horseshoe time, tadpole time, and AV vs. inclination for sample leg (tour 2, leg 19)

Alternatively, a strategy of avoiding only tbc inner icy satellites' tadpole regions could be chosen. Crossings of these regions occur on 1() legs in tour 1. An estimated 1O m/s is required to avoid the crossings on each of these legs, for a total of 100 m/s.

Table 7 shows results calculated for the the other sample tours in a similar fashion. Although these AV estimates are preliminary, it is clear that the AV cost of using broken-plane maneuvers to keep inclination near the minimum value needed to clear all horseshoe and tadpole zones is expensive, perhaps prohibitive,

Another strategy is to avoid both the horseshoes and tadpoles of the inner icy satellites for only the first two years while evaluating the debris hazard in-situ, instead of committing beforehand to avoiding them for the entire tour'. Estimates of AV costs 10 do this for the sample tours are also shown in Table **7.**

Table 7
ESTIMATES OF AV COST IN M/S TO AVOID HORSESHOES & TADPOLES OF INNER ICY SATELLITES
(HS=horseshoe, TP=Tadpole)

	Avoid for entire tour		Avoid for 1st 2 yr.	
TOUR	HS+TP	TP only	HS+TP	TP only
1	480	100	220	40
2	260	40	60 '	10
3	280	20	60	10
4	340	0	160	20
5	400	60	?60	40
6	160	10	60 '	10

* Repeated crossings of Dione's horseshoe between T5 and T6 because one of the two nodes is at Dione's orbit. These crossings can be eliminated by using a cliff erent period/ periapse combination on that orbit, requiring no AV expenditure.

Tours 2, 3 and 6 illustrate a strategy which avoids the inner icy satellites' horseshoes and tadpoles for the first two years at comparatively low AV cost. Broken-plane maneuvers arc needed only to eliminate the crossings represented by the first two vertical bars in the horseshoe plots of Figure *7,* associated with the T? and T3 flybys. These crossings occur as inclination is lowered to near the equator to allow the spacecraft to hop from an inbound to an outbound Titan flyby, In both of these tours, the spacecraft spends the rest of the first two years at high inclinations, using 360° transfers to raise and lower inclination (and, in the case of tour 6, to set up the conditions required to accomplish the. 1800 transfer). A 180° transfer allows us to avoid horseshoe and tadpole zones early in the tour at low AV cost while accomplishing substantial orbit rotation. No net orbit rotation is accomplished by Titan flybys if only 3600 transfers are used.

AVOIDING TITAN'S ZONES

Avoiding Titan's horseshoes and tadpoles is not always feasible, because one of the spacecraft's orbital nodes must always be near Titan's orbit in order to be able to achieve a high number of Titan flybys in the tour. Nevertheless, some crossings of Titan's zones occur in near-cqu:itorial orbits, far from a node, These can be eliminated using the strategies discussed above (180°/3600 transfers, broken-plane maneuvers) to increase inclination.

The leg between Titan 9 and Titan 11 of tour 1 shows how some Titan zone passages can be avoided and some cannot. Titan 9 is inbound and Titan1 1 is outbound, with more than two complete revs between them. This leg is near-equatorial, with an inclination of 0.3°. Four Titan horseshoe passages occur (one inbound and one outbound on each of the two complete revs between the flybys). We can eliminate the two outbound horseshoe passages by using Titan 9 to increase inclination and adding a broken-plane maneuver at the second apoapsis after Titan 9. However, in doing so, we establish a node at the point in Titan's orbit where the Titan 9 flyby takes place (i.e., inbound, on the spacecraft's orbit). The spacecraft

passes through Titan's horseshoe al that point twice before the maneuver changes its orbit, targeting to Titan 11. If instead we place the maneuver at the first post-Titan 9 apoapsis, wc establish the node outbound, preserving the outbound horseshoe passages but eliminating the inbound ones. Selected events on this leg arc listed in Table 8.

Table 8
SELECTED EVENTS BETWEEN TITAN 9 AND TITAN 11, TOUR 1

Event	True Anomaly	Event	True Anomaly
Titan 9	–131°	1 itan horseshoe	131"
Periapsis	0"	Apoapsis	180°
Apoapsis	180°	1 itan horseshoe	-133°
Titan horseshoe	–133°	F 'eriapsis	0°
Periapsis	0°	1 itan 11	128°

Because the radii of Titan's zones are large.r than those of the icy satellites, broken-plane maneuvers must be larger to avoid them (in cases where they can be avoided). About 60 m/s is needed to avoid Titan's horseshoe; about 30 m/s is needed to avoid Titan's tadpole.

The number of crossings of Titan's tadpoles at high inclination can be minimized by minimizing the number of times the spacecraft travels more than three revolutions between Titan flybys (see Table 6). This could mean reducing the number of equatorial Saturn/ring occultations in the tour. in the sample tours, legs of five revolutions between flybys are used to obtain five such occultations (one per spacecraft revolution) after establishing the inclination which yields occultations. If wc reduce the number of spacecraft revolutions to three, we achieve only three occultations,

Titan's tadpole zones cannot be completely avoided unless inclination is limited to about 65° or less. In general, the lower the orbital period, the higher the maximum inclination which can bc achieved. Given the constraint that periapse must be greater than 2.7 RS, the lowest orbital period achievable with three spacecraft revolutions is 10.6 days (three spacecraft revolutions : two Titan revolutions) which limits us to this maximum inclination. Higher inclinations can only be achieved at lower orbital periods which necessitate more than three spacecraft revolutions between flybys. Inclinations of 70°-800 are typically achieved at orbital periods of 7.1 days (nine spacecraft revolutions : four Titan revolutions). The relationship between period and maximum inclination is discussed in greater detail in Ref. 19.

Table 9 presents some rough guesstimates of how much the amount of time spent in Titan's horseshoes and tadpoles could be reduced by applying the. above methods for the sample tours.

Table 9
PRELIMINARY ESTIMATE OF POTENTIAL REDUCTION IN TITAN HORSESHOE AND TADPOLE ZONE EXPOSURE (WITH AV NEEDED TO ACHIEVE REDUCTION)

		HORSESHOES (hrs.)			TADPOLES (hrs.)	
		Time			Time	
Tour	ΔV (m/s)	Eliminated	Remaining	AV (m/s)	Eliminated	Remaining
1	540	44	189	180	16	**26**
2	120	21	68	60	3	**4**
3	240	16	179			**26**
4	420	36	90	0	4	**11**
5	480	32	138			**18**
6	240	24	195	0	4	41

CONCLUSIONS

Analysis of the restricted three-body problem produces regions shaped like horseshoes and tadpoles along the satellites' orbits within which particles can be trapped. Voyager observed three objects trapped near the orbits of Tethys and Dione; however, little is known about the actual debris populations of horseshoe or tadpole zones. In six sample Cassini tours evaluated using homogeneous particle density models for the E ring, the probability of an impact with a particle trapped in one of these zones causing mission failure or significant degradation was found to be negligible. However, continuing efforts are being made to model particle sizes in horseshoe and tadpole regions using microsignatures, theoretical analysis, and edge-on ring observations.

In recognition of the large uncertainties in the particle models, strategies of avoiding these zones were explored. The amount of time the spacecraft spends in these regions depends strongly on orbital geometry in the tour. Large reductions in the time spent in the inner icy satellites' zones can be accomplished by keeping inclination above about 2°, using 360° or 180° transfers, or broken-plane maneuvers (for transfer angles of other than 180° or 3600). The necessity of encountering, Titan frequently makes avoiding Titan's zones impossible in many cases. However, Titan lies outside the E ring, which is the presumed source of most particles of concern. Tradeoffs associated with avoiding these zones involve model uncertainties, tour strategies, science observations, and AV cost. These tradeoffs must be evaluated carefully, and efforts to reduce model uncertainties should be undertaken when possible.

ACKNOWLEDGEMENTS

The invaluable assistance of Andrey Sergeyevsky on zero-velocity contours and the three-body problem, as well as his assistance in producing and evaluating STOUR results, is gratefully acknowledged. This work was performed at the Jet Propulsion Laboratory, California Institute of Technology, under contract with the National Aeronautics and Space Administration.

REFERENCES

1. Cassini Mission Plan, Revision F. April 1, 1995, JPL D-5564.

2. Showalter, M. R., Cuzzi, J. N., and Larson, S.M, Structure anti Particle Properties of Saturn's E Ring. *Icarus* 94,451-473 (1991).

3. Roy, A. E., *Orbits/ Motion.* 1978, Halstead Press, New York.

4. Szebehely, V., *Theory of Orbits - The Restricted Problem of Three Bodies.* 1967, Academic Press, New York.

5. Dermott, S. F., and Murray, C. D., The Dynamics of Tadpole and Horseshoe Orbits (2 parts). *Icarus 48,* 1-11 and 12-22, 1981

6. Zhao, Z-Y., and Liu, L., I-he Stable Regions of the Triangular Libration Points of the Planets. */car'us* 100, 136-142, 1992

7. Bender, D. F., "Relative Motion Among the Trojan Asteroids", Paper #DPS 31.1 3-P, presented at the DPS conference, Washington, D. C., Ott/Nov, 1994

8. Seidelmann, P. K., Barrington, R. S., and Szebehely, V., Dynamics of Saturn's E Ring. *Icarus* 58, 169-177, 1984

9. Feibelman, W. A., Concerning the 'D' Ring of Saturn. *Nature* 214, 793-794, 1967

10. Baum, W. A., Kreidl, T., Westphal, J. A., Danielson, G. E., Seidelmann, P. K., and Pascu, D. Saturn's E Ring. *Icarus* 47, 84-96, 1981

11. Haff, P. K., Eviatar, A., and Siscoe, G. L., Ring and Plasma: The Enigmae of Enceladus. *Icarus* 56, 426-438, 1983

12. Sinclair, A.T., Perturbations on the orbits of companions of the satellites of Saturn. *Astron. Astrophys.* 136, 161-166, 1984

13. Pang, K. D., Voge, C. C., Rhoads, J. W., and Ajello, **J. M.,** The E Ring of Saturn and Satellite Enceladus. Paper # 4B0886, American Geophysical Union, 1984

14. Divine, N., "Risk Analysis for Saturn Ring Particles Impacting the Cassini Orbiter," JPL IOM 5217-89-153, October 2, 1989

15. Burns, J. A., Kolvoord, R. A., and Hamilton, D. P., "An Assessment of Potential Hazards to the Cassini Spacecraft from Debris along Satellite Orbits", Report to Cassini Project, August 1989

16. Divine, N., "Particle Distributions in the Orbits of Five Saturn Satellites," JPL IOM 5217-90-129, October 9, 1990

17. Wolf, A. A., and Byrnes, D. V., "Design of the Galileo Satellite Tour", AAS Paper #93-567, presented at the AAS/AIAA Astrodynamics Specialist conference, Victoria, B. C., Canada, Aug. 1993

18. Uphoff, Roberts, and Friedman, "Orbit Design Concepts for Jupiter Orbiter Missions", AIAA Paper #74-781, presented at the AIAA Mechanics and Control of Flight Conference, Anaheim, CA, Aug. 1974

"19. Wolf, A. A., "Maximizing Inclination in Cassini Tours," JPL IOM 312/94.4-2058, 2 Sept., 1994